Antinuclei from Primordial Black Holes

Based on 2505.04692 - Phys. Rev. D 112 (2025) 2, 023003

in collaboration with V. De Romeri, F. Donato, D. Maurin & L. Stefanuto

Agnese Tolino

IFIC (CSIC-UV)

PASCOS 2025 – Durham, UK

July 22nd, 2025

2505.04692
Phys. Rev. D 112 (2025) 2, 023003

OUR WORK IN A NUTSHELL

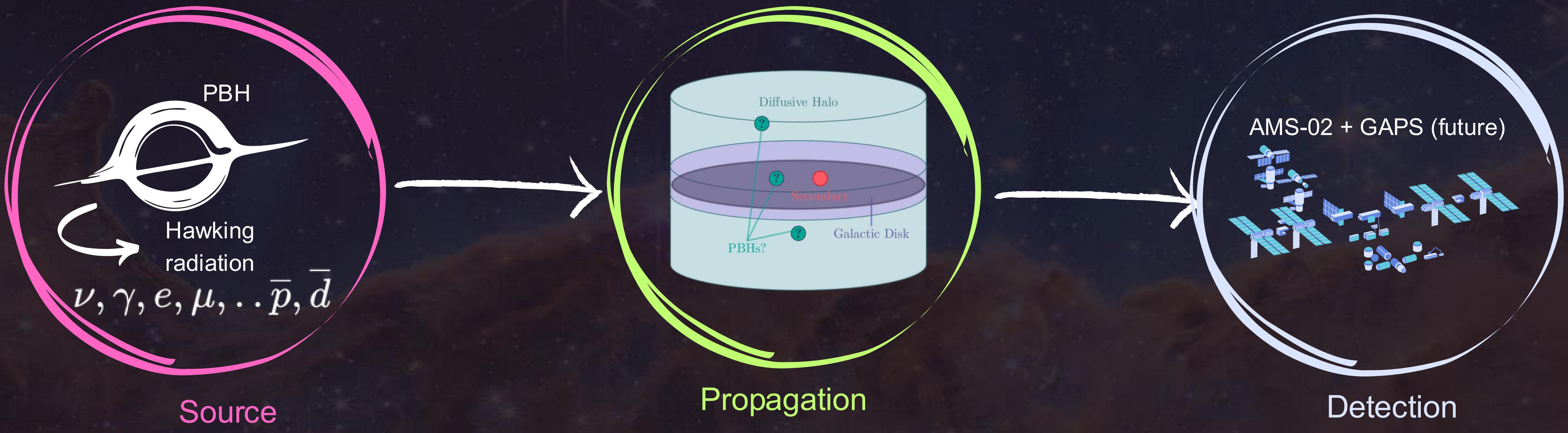

We estimated the **antiproton** and **antideuteron signals** from a population of Schwarzschild **primordial black holes** (PBHs) following a **lognormal** mass distribution. By comparing with AMS-02 data, we derived competitive **constraints** on the fraction of dark matter that such PBHs could account for and discussed **perspectives** for antideuteron measurements with AMS-02 and GAPS

See also:
J. Herms et al., JCAP 02 (2017)
A. Barrau et al., Astron. Astrophys. 388 (2002) 676
A. Barrau et al. Astron. Astrophys. 398 (2003) 403

PRIMORDIAL BLACK HOLES

Source

- Might have formed in the Early Universe by the collapse of large density fluctuations

Hawking, Nature 248 (1974) 30-31
Carr et al., Ann. Rev. Nucl. Part. Sci. 70 (2020)
Carr et al., Rept. Prog. Phys. 84 (2021) 11, 116902

PRIMORDIAL BLACK HOLES

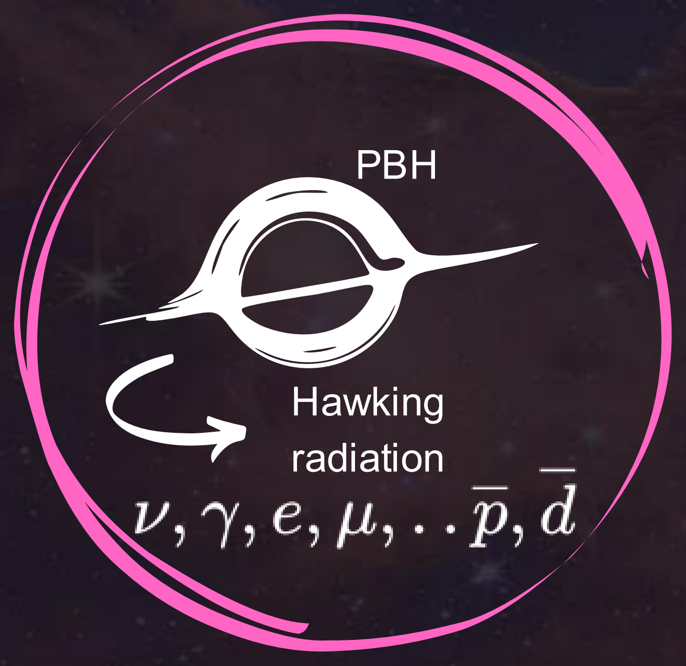

Source

- Might have formed in the Early Universe by the collapse of large density fluctuations
- Uniquely described by mass, charge and angular momentum
  - Schwarzschild PBH: non-rotating and uncharged

Hawking, Nature 248 (1974) 30-31
Carr et al., Ann. Rev. Nucl. Part. Sci. 70 (2020)
Carr et al., Rept. Prog. Phys. 84 (2021) 11, 116902

PRIMORDIAL BLACK HOLES

Source

- Might have formed in the Early Universe by the collapse of large density fluctuations
- Uniquely described by mass, charge and angular momentum
  - Schwarzschild PBH: non-rotating and uncharged
- Masses span from 10^{-5}g to $10^5 M_\odot$

Hawking, Nature 248 (1974) 30-31
Carr et al., Ann. Rev. Nucl. Part. Sci. 70 (2020)
Carr et al., Rept. Prog. Phys. 84 (2021) 11, 116902

PRIMORDIAL BLACK HOLES

Source

- Might have formed in the Early Universe by the collapse of large density fluctuations
- Uniquely described by mass, charge and angular momentum
  - Schwarzschild PBH: non-rotating and uncharged
- Masses span from 10^{-5} g to $10^{5} M_{\odot}$
- PBHs above 5×10^{14} g could be viable DM candidates, as they would have not completely evaporated yet

Hawking, Nature 248 (1974) 30-31
Carr et al., Ann. Rev. Nucl. Part. Sci. 70 (2020)
Carr et al., Rept. Prog. Phys. 84 (2021) 11, 116902

HAWKING RADIATION…

- Hawking predicted that (Schwarzschild) PBHs evaporate with a temperature

$$T = \frac{1}{8\pi G M_{\rm PBH}}$$

- Mass loss goes as

$$\frac{dM}{dt} \sim M_{\rm PBH}^{-2}$$

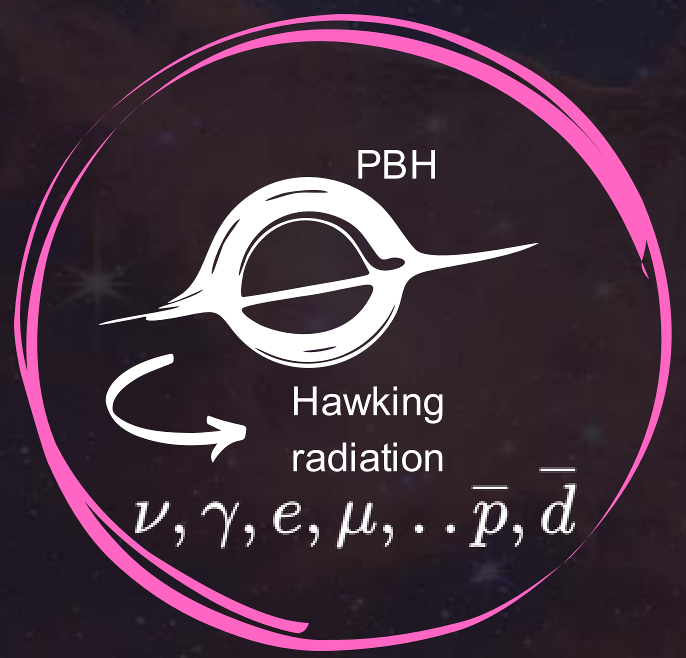

Source

Hawking, Nature 248 (1974) 30-31
Carr et al., Ann. Rev. Nucl. Part. Sci. 70 (2020)
Carr et al., Rept. Prog. Phys. 84 (2021) 11, 116902
Arbey et al., Eur. Phys. J. C 79 no. 8, (2019) 693
Barrau, et al., Astron. Astrophys. 388 (2002) 676
Herms et al.l, JCAP 02 (2017) 018

HAWKING RADIATION...

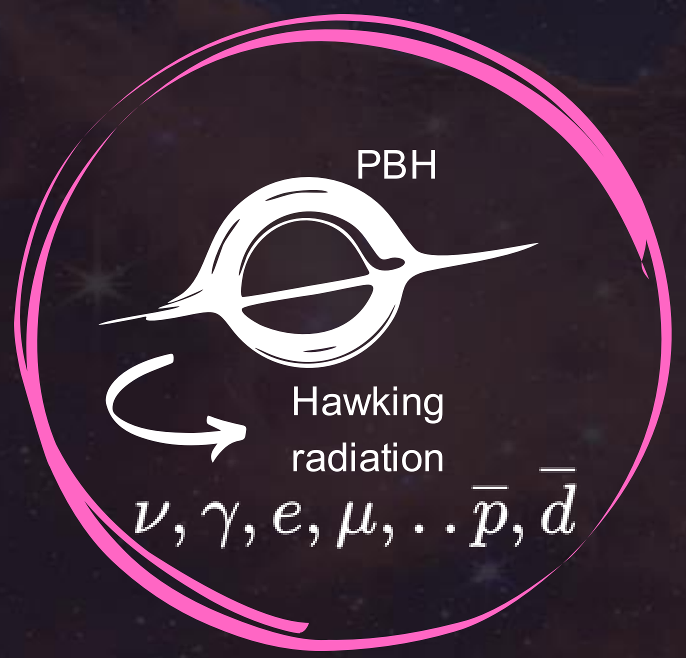

Source

- Hawking predicted that (Schwarzschild) PBHs evaporate with a temperature

$$T = \frac{1}{8\pi G M_{\mathrm{PBH}}}$$

- Mass loss goes as

$$\frac{dM}{dt} \sim M_{\mathrm{PBH}}^{-2}$$

- The evaporation corresponds to the emission of (fundamental) particles with a semi-black body spectrum

$$\left.\frac{dN^i}{dEdt}\right|_{\mathrm{prim}} = \frac{g_i \Gamma\left(M_{\mathrm{PBH}}, E_i\right)}{2\pi\left(\exp\left\{\frac{E_i}{T_{\mathrm{PBH}}}\right\} - (-1)^{2s_i}\right)}$$

- Any fundamental (leptons, bosons, quarks… maybe DM!) particle can be emitted as long as $m_i \leq T_{PBH}$

Hawking, Nature 248 (1974) 30-31
Carr et al., Ann. Rev. Nucl. Part. Sci. 70 (2020)
Carr et al., Rept. Prog. Phys. 84 (2021) 11, 116902
Arbey et al., Eur. Phys. J. C 79 no. 8, (2019) 693
Barrau, et al., Astron. Astrophys. 388 (2002) 676
Herms et al.l, JCAP 02 (2017) 018

… AND ANTIPARTICLES

- **Antiprotons** and **antideuterons** are not directly emitted by the PBH

Source

Hawking, Nature 248 (1974) 30-31
Carr et al., Ann. Rev. Nucl. Part. Sci. 70 (2020)
Carr et al., Rept. Prog. Phys. 84 (2021) 11, 116902
Arbey et al., Eur. Phys. J. C 79 no. 8, (2019) 693
Barrau, et al., Astron. Astrophys. 388 (2002) 676
Herms et al.l, JCAP 02 (2017) 018

… AND ANTIPARTICLES

- **Antiprotons** and **antideuterons** are not directly emitted by the PBH
- Indeed, antiprotons result from the **EW processes** and/or **hadronization** of mainly quarks and bosons directly emitted through Hawking radiation

Source

$\bar{p}$

Hawking, Nature 248 (1974) 30-31
Carr et al., Ann. Rev. Nucl. Part. Sci. 70 (2020)
Carr et al., Rept. Prog. Phys. 84 (2021) 11, 116902
Arbey et al., Eur. Phys. J. C 79 no. 8, (2019) 693
Barrau, et al., Astron. Astrophys. 388 (2002) 676
Herms et al.l, JCAP 02 (2017) 018

… AND ANTIPARTICLES…

- **Antideuterons** are formed through the **coalescence** of an antiproton with an antineutron

Source

C. Arina et al, 2312.01153
M. Cirelli et al., JCAP 03 (2011) 051
M. Di Mauro et al., 2411.04815

... AND ANTIPARTICLES...

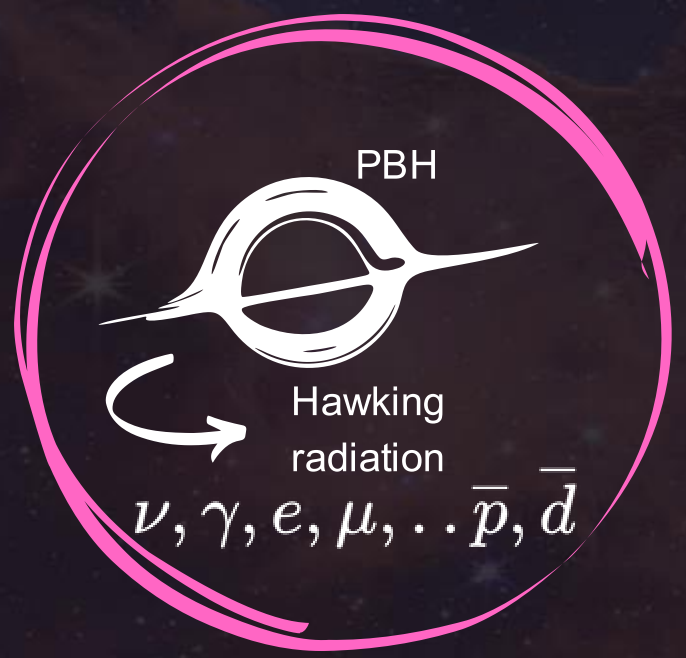

Source

- **Antideuterons** are formed through the **coalescence** of an antiproton with an antineutron
- Basic models fix a max. momentum for the coalescence, tuned on ALEPH data (e+e- Z resonance)

C. Arina et al, 2312.01153
M. Cirelli et al., JCAP 03 (2011) 051
M. Di Mauro et al., 2411.04815
ALEPH collaboration, PLB 639, 3–4, 2006

… AND ANTIPARTICLES…

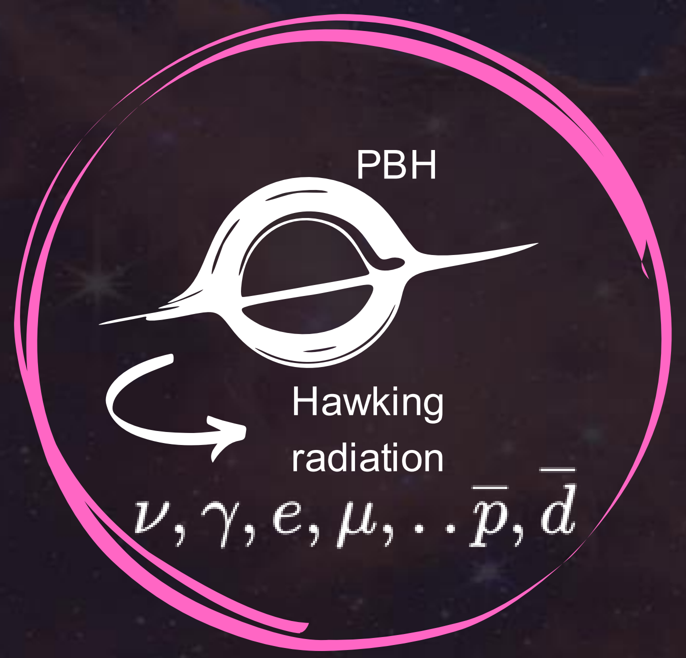

Source

- **Antideuterons** are formed through the **coalescence** of an antiproton with an antineutron

- Basic models fix a max. momentum for the coalescence, tuned on ALEPH data (e+e- Z resonance)

- More sophisticated models: Argonne-Wigner
  considers the antinuclei density matrices to estimate the coalescence ***probability*** *(Wigner formalism) & an Argonne-like potential for the antideuteron*

C. Arina et al, 2312.01153
M. Cirelli et al., JCAP 03 (2011) 051
M. Di Mauro et al., 2411.04815
ALEPH collaboration, PLB 639, 3–4, 2006
M. Mahlein et al., Eur. Phys. J. C 83, 804 (2023)
R.B. Wiringa et al., Phys. Rev. C 51, 38 (1995)

... AND ANTIPARTICLES...

Source

- **Antideuterons** are formed through the **coalescence** of an antiproton with an antineutron

- Basic models fix a max. momentum for the coalescence, tuned on ALEPH data (e+e- Z resonance)

- More sophisticated models: Argonne-Wigner

  considers the antinuclei density matrices to estimate the coalescence probability (Wigner formalism) & an Argonne-like potential for the antideuteron

- **CosmiXs:** tool to evaluate antiproton and antideuteron production from quarks and bosons

C. Arina et al, 2312.01153
M. Cirelli et al., JCAP 03 (2011) 051
M. Di Mauro et al., 2411.04815
ALEPH collaboration, PLB 639, 3–4, 2006
M. Mahlein et al., Eur. Phys. J. C 83, 804 (2023)
R.B. Wiringa et al., Phys. Rev. C 51, 38 (1995)

...AND EXTENDED MASS DISTRIBUTIONS

- In general, PBHs can all have one mass (monochromatic) or follow extended mass distributions when formed

Source

M.R. Mosbech et al., SciPost Phys. 13 (2022) 100
Herms et al.l, JCAP 02 (2017) 018

...AND EXTENDED MASS DISTRIBUTIONS

- In general, PBHs can all have one mass (monochromatic) or follow extended mass distributions when formed

- For example, they can follow a lognormal mass distribution for PBHs at the formation time with critical mass μ_c and width σ

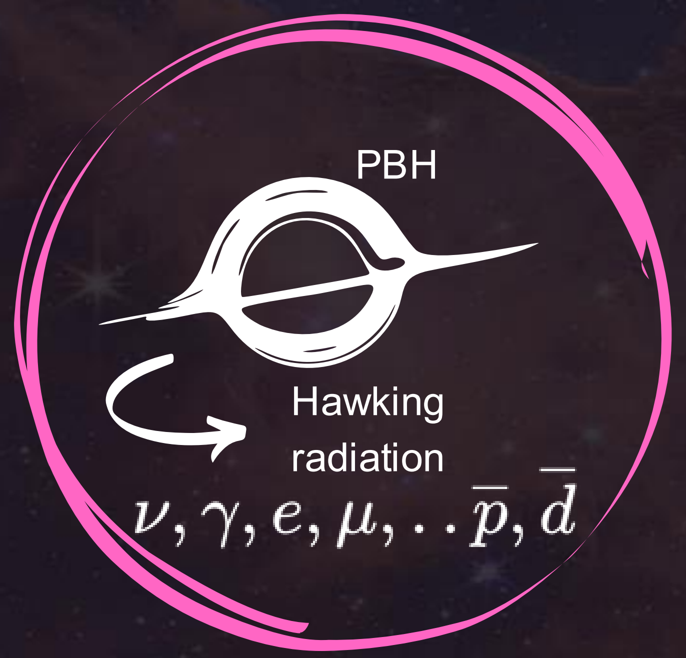

Source

M.R. Mosbech et al., SciPost Phys. 13 (2022) 100
Herms et al.l, JCAP 02 (2017) 018

…AND EXTENDED MASS DISTRIBUTIONS

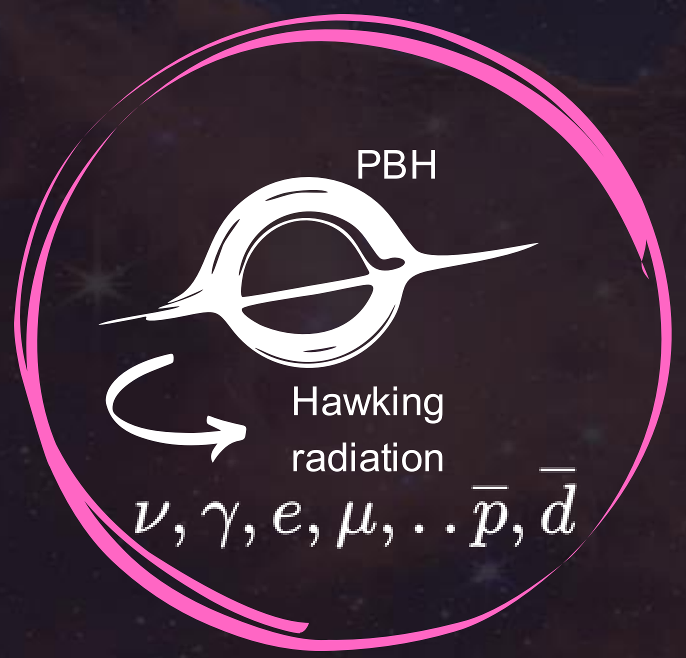

Source

- In general, PBHs can all have one mass (monochromatic) or follow extended mass distributions when formed
- For example, they can follow a lognormal mass distribution for PBHs at the formation time with critical mass μ_c and width σ
- However, extended PBH distributions are affected by the time evolution of the PBH and hence will change through time

$$\frac{g(M)}{M} = \frac{dn_{\mathrm{PBH}}}{dM} = \frac{dn_{\mathrm{PBH}}}{dM_{\mathrm{in}}}\frac{dM_{\mathrm{in}}}{dM} = \rho_{\mathrm{PBH}}(r,z)\frac{\mathcal{A}}{\sqrt{2\pi}\sigma M_{\mathrm{in}}^2}\exp\left[-\frac{\log^2(M_{\mathrm{in}}/\mu_c)}{2\sigma^2}\right]\frac{M^2\alpha(M_{\mathrm{in}})}{M_{\mathrm{in}}^2\alpha(M)},$$

M_{in} initial PBH mass at formation

M PBH mass at the age of the universe

α evaporation coefficient

ρ_{PBH} PBH density in the (r,z) cylinder

M.R. Mosbech et al., SciPost Phys. 13 (2022) 100
Herms et al.l, JCAP 02 (2017) 018

...AND EXTENDED MASS DISTRIBUTIONS

Source

- In general, PBHs can all have one mass (monochromatic) or follow extended mass distributions when formed
- For example, they can follow a lognormal mass distribution for PBHs at the formation time with critical mass μ_c and width σ
- However, extended PBH distributions are affected by the time evolution of the PBH and hence will change through time

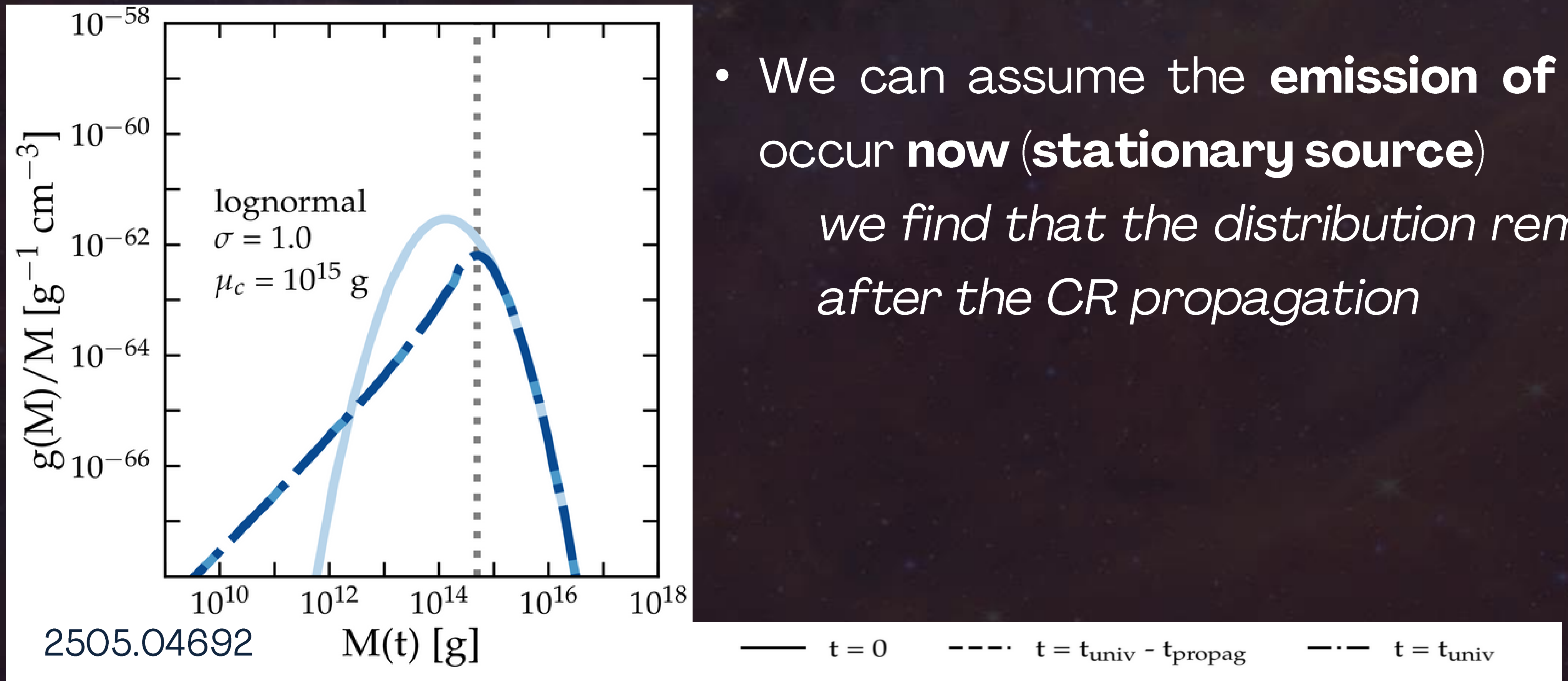

- We can assume the **emission of antinuclei** by PBHs to occur **now** (**stationary source**)

  we find that the distribution remains almost unchanged after the CR propagation

M.R. Mosbech et al., SciPost Phys. 13 (2022) 100

Herms et al.l, JCAP 02 (2017) 018

COSMIC RAYS PROPAGATION

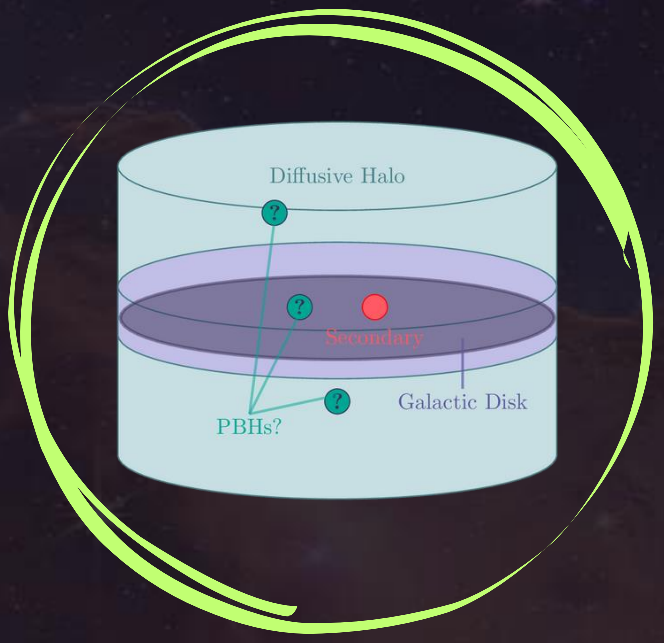

Propagation

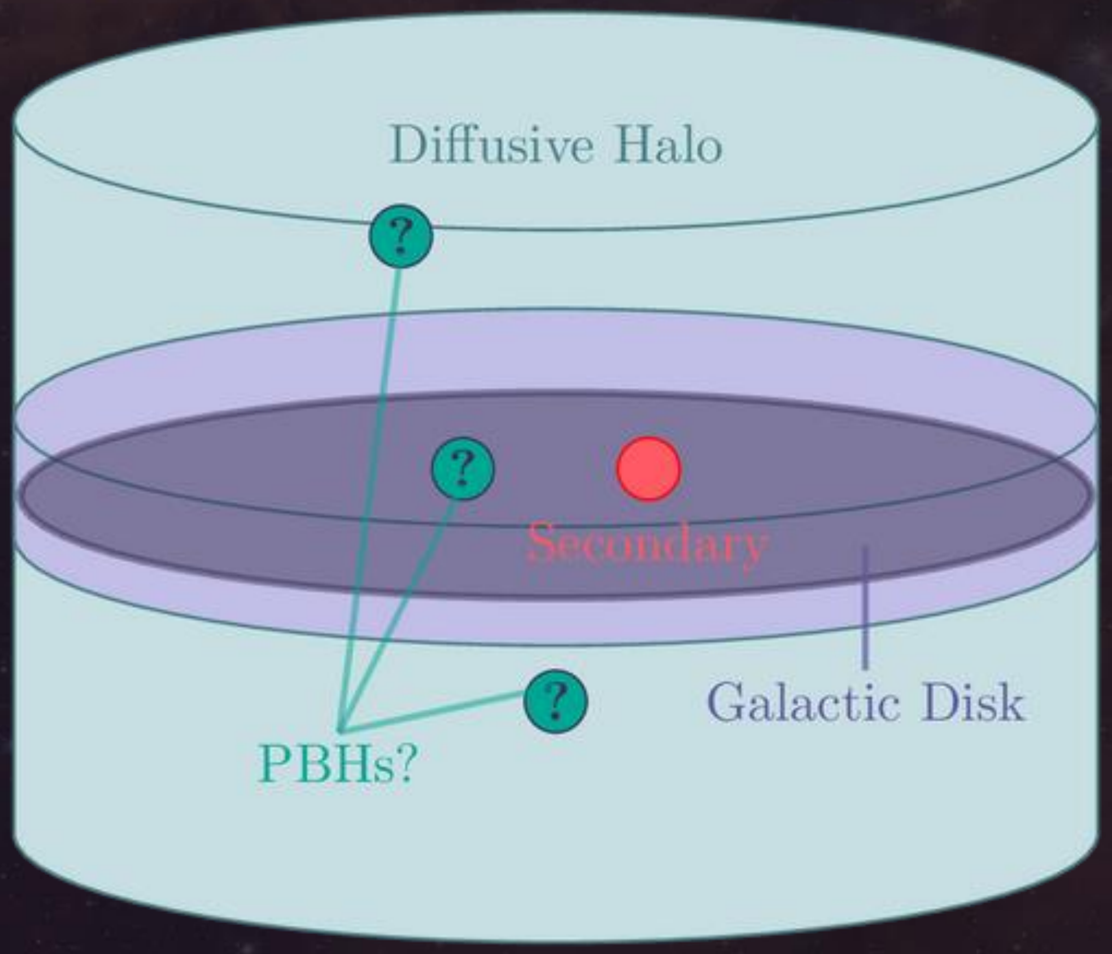

- The Galaxy is a thin disk surrounded by inhomogeneous magnetic fields, that cause **cosmic rays** (**CRs**) to diffuse in the so-called diffusive halo

V.S. Berezinskii, et al., *Astrophysics of cosmic rays*, Elsevier Science and Technology (1990)
Y. Genolini et al., Phys. Rev. D 99 (2019) 123028

COSMIC RAYS PROPAGATION

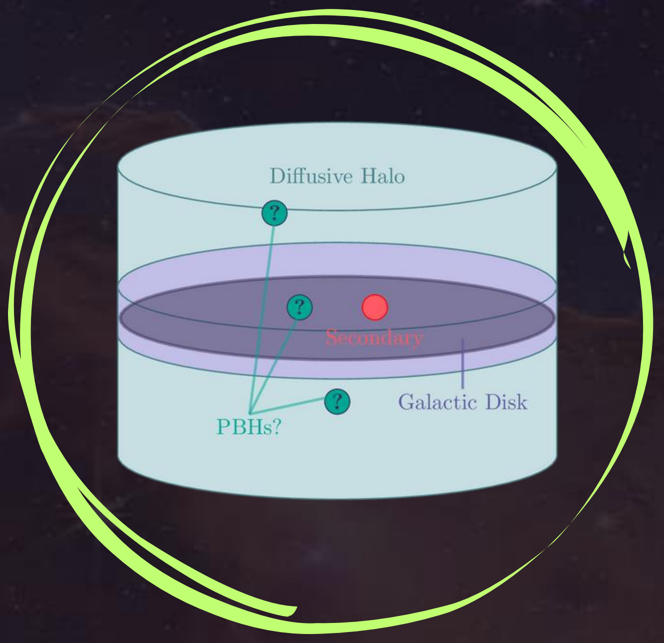

Propagation

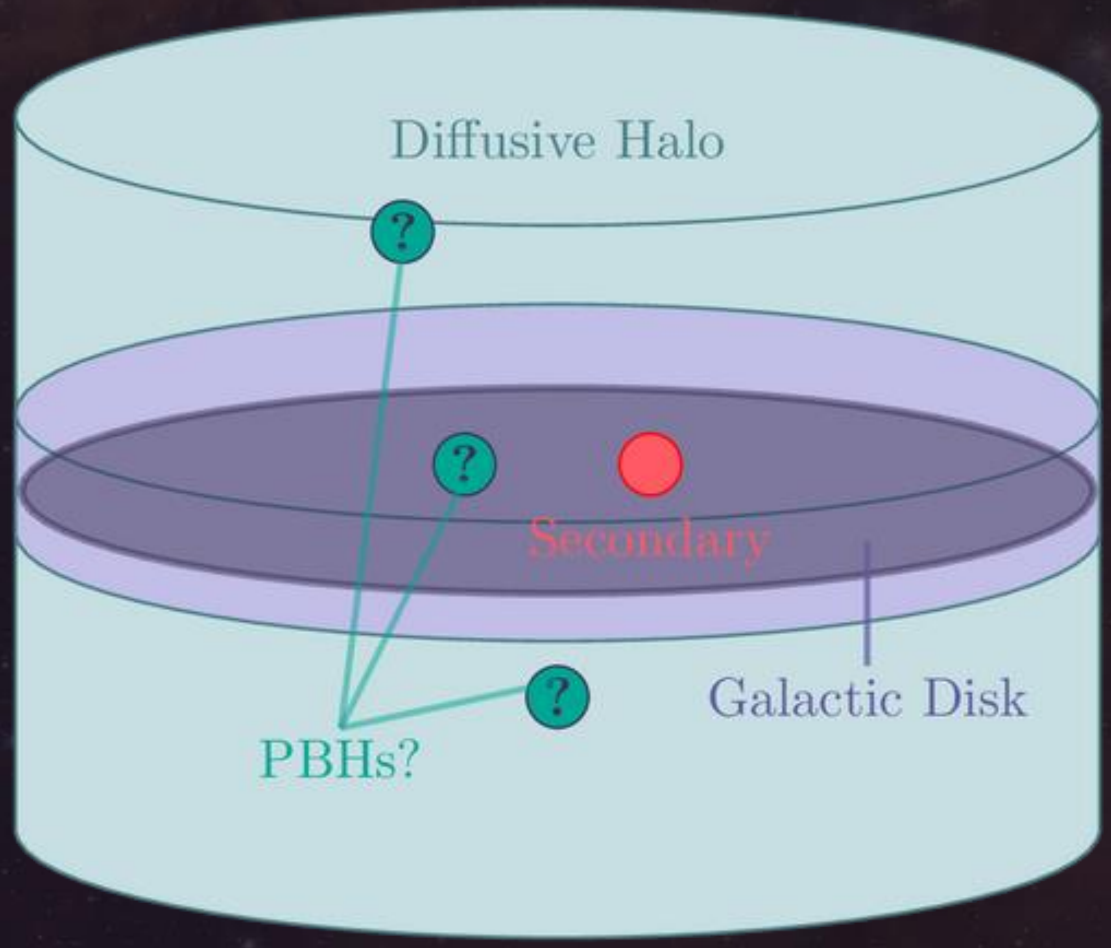

- The Galaxy is a thin disk surrounded by inhomogeneous magnetic fields, that cause **cosmic rays** (**CRs**) to diffuse in the so-called diffusive halo
- PBHs could be **located** anywhere **in the diffusive halo**

V.S. Berezinskii, et al., *Astrophysics of cosmic rays*, Elsevier Science and Technology (1990)
Y. Genolini et al., Phys. Rev. D 99 (2019) 123028

COSMIC RAYS PROPAGATION

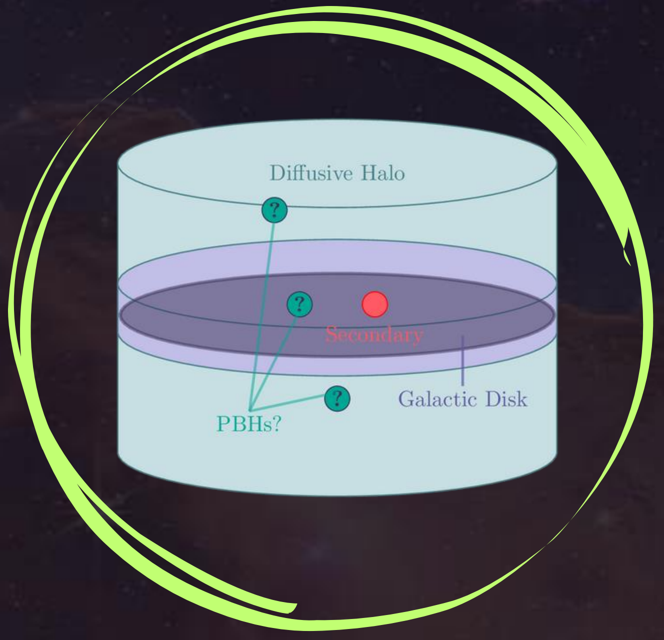

Propagation

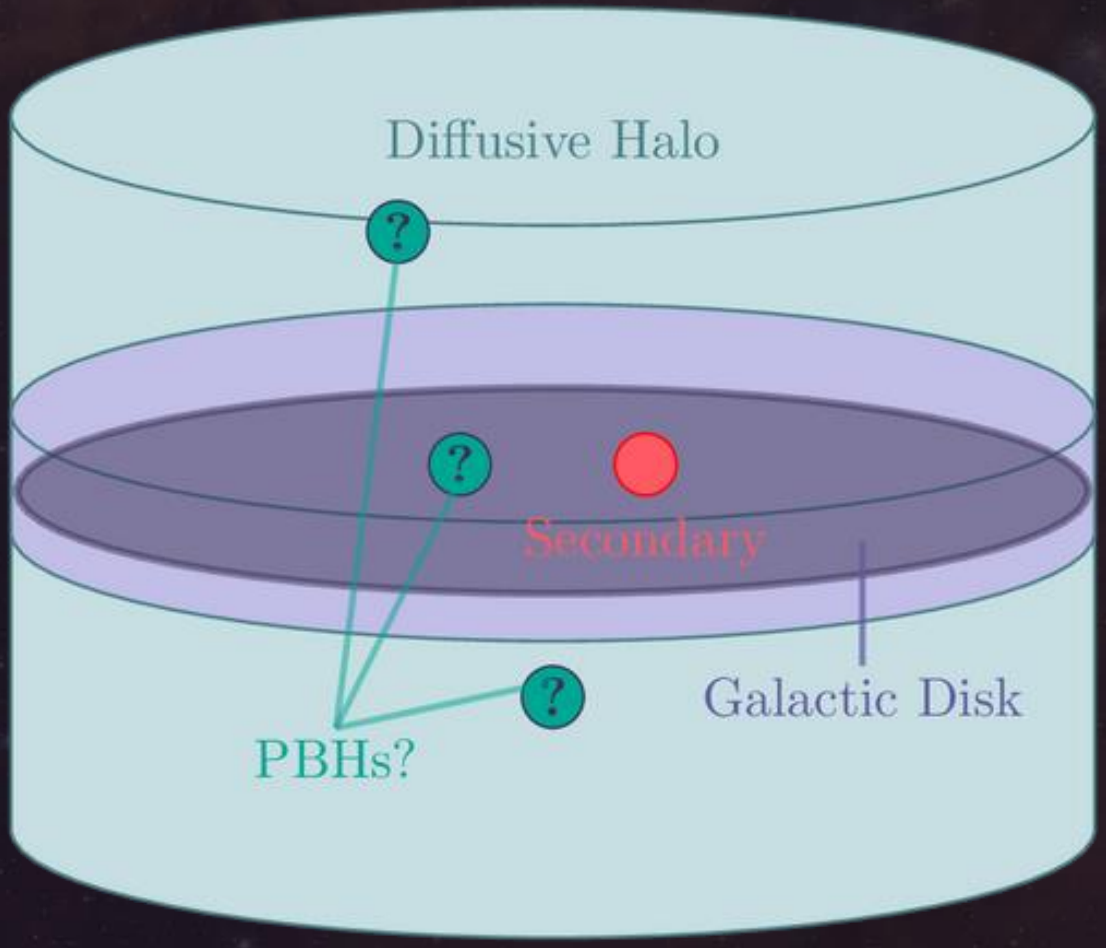

- The Galaxy is a thin disk surrounded by inhomogeneous magnetic fields, that cause **cosmic rays** (**CRs**) to diffuse in the so-called diffusive halo
- PBHs could be **located** anywhere **in the diffusive halo**
- Once produced by PBHs, the antinuclei **propagate** and arrive to the Earth

V.S. Berezinskii, et al., *Astrophysics of cosmic rays*, Elsevier Science and Technology (1990)
Y. Genolini et al., Phys. Rev. D 99 (2019) 123028

COSMIC RAYS PROPAGATION

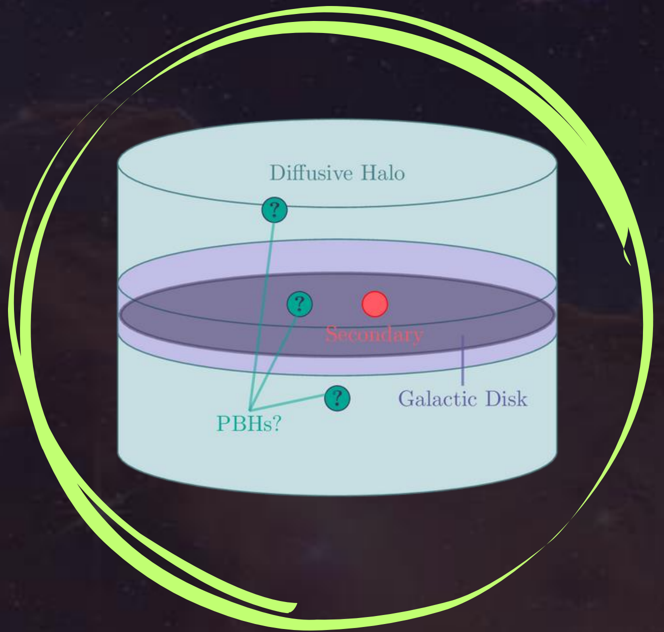

Propagation

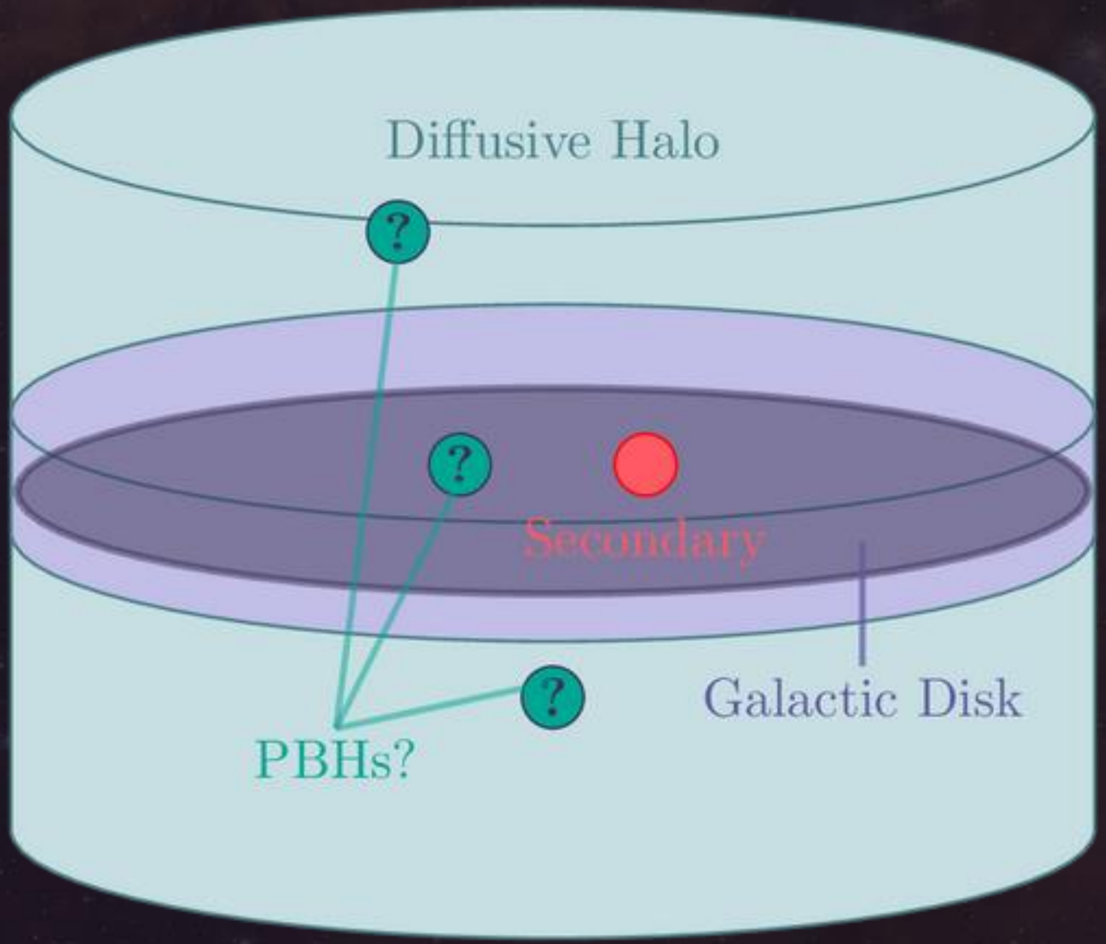

- The Galaxy is a thin disk surrounded by inhomogeneous magnetic fields, that cause **cosmic rays** (**CRs**) to diffuse in the so-called diffusive halo
- PBHs could be **located** anywhere **in the diffusive halo**
- Once produced by PBHs, the antinuclei **propagate** and arrive to the Earth
- In addition to this, **secondary antinuclei** are produced by the **spallation of primary** (mainly from supernovae shock waves) CRs over the H and He in the Galactic disk

V.S. Berezinskii, et al., *Astrophysics of cosmic rays*, Elsevier Science and Technology (1990)
Y. Genolini et al., Phys. Rev. D 99 (2019) 123028

COSMIC RAYS PROPAGATION

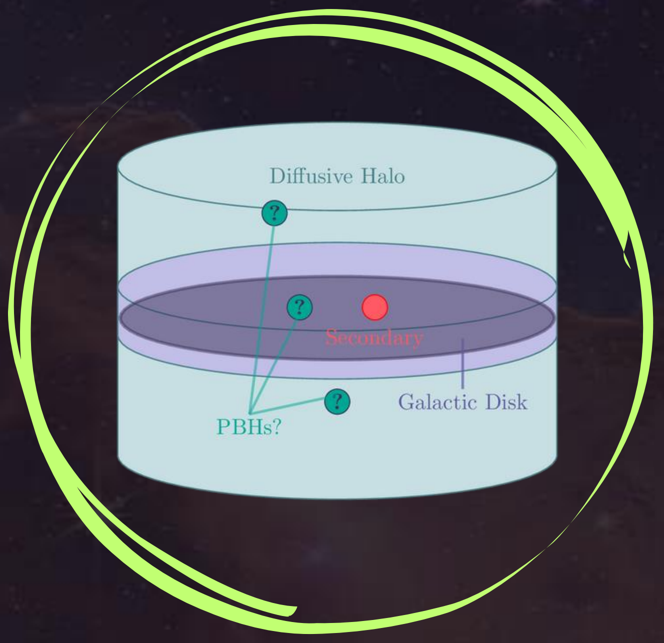

Propagation

- Different propagation (or *transport*) configurations (L, R, h...)
  - Most "complete one": BIG, with low-rigidity break of the spatial diffusion, reacceleration, convective wind...

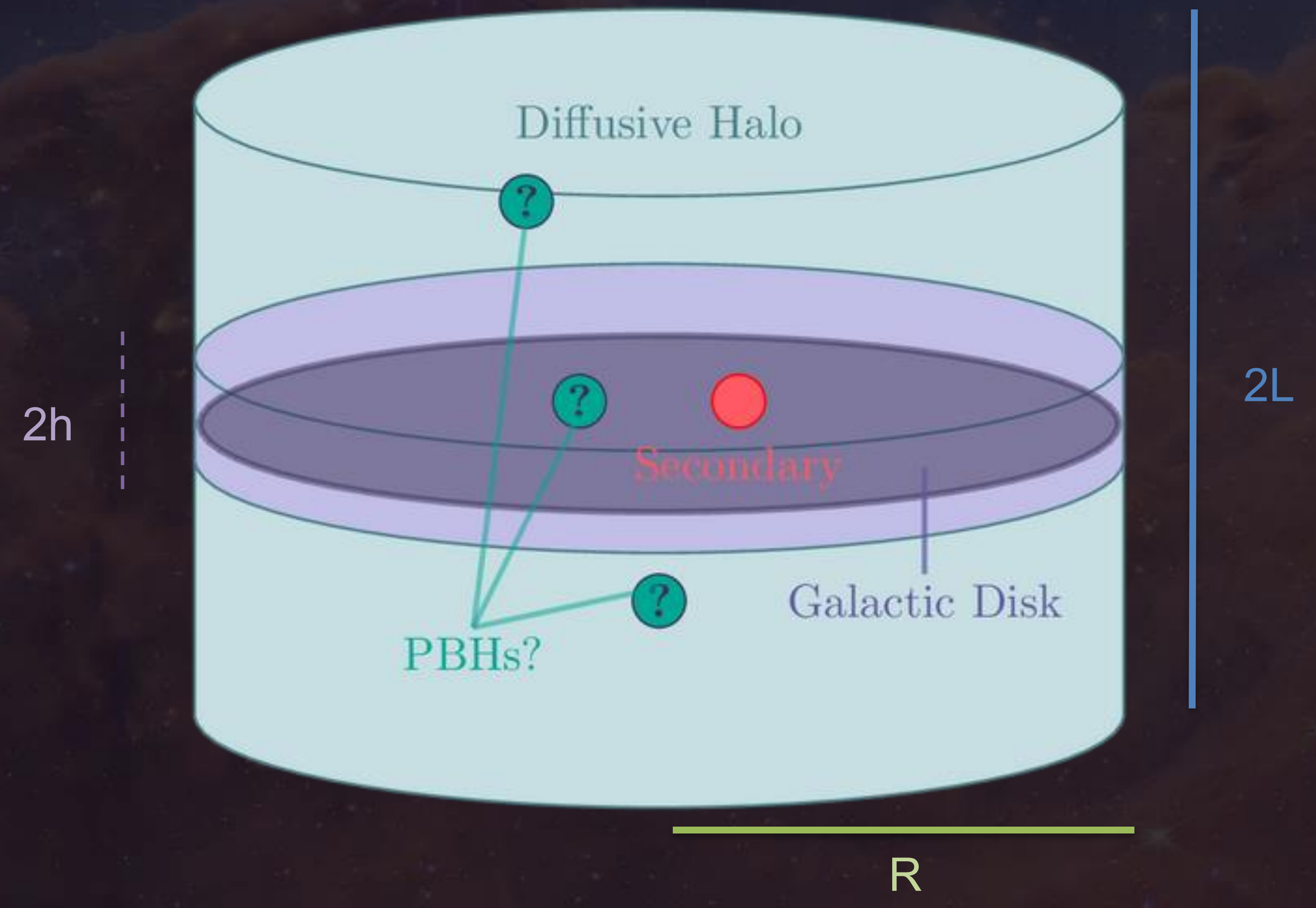

V.S. Berezinskii, et al., *Astrophysics of cosmic rays*, Elsevier Science and Technology (1990)
Y. Genolini et al., Phys. Rev. D 99 (2019) 123028

AMS-02 & GAPS: DETECTING ANTINUCLEI

- The **Alpha Magnetic Spectrometer** (**AMS**) detector is designed to operate as an external module on the ISS

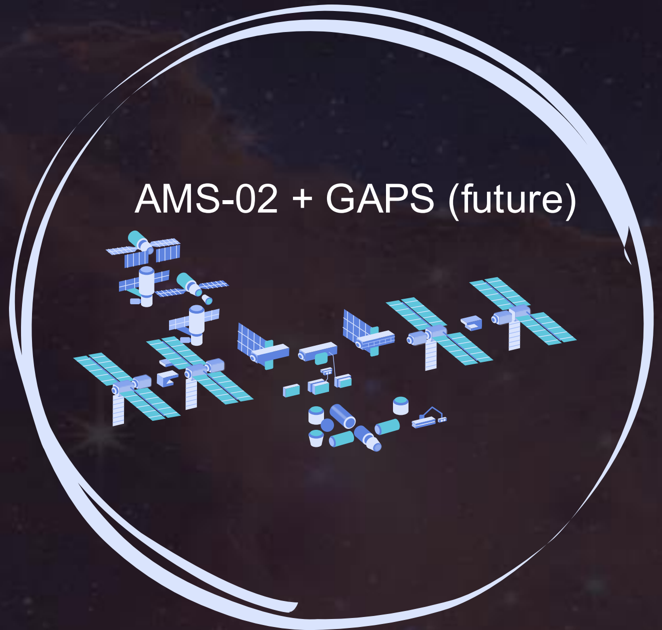

Detection

AMS collaboration, Phys. Rev. Lett. 117 (2016) 091103
AMS collaboration, Phys. Rept. 894 (2021)
T. Aramaki et al., GAPS, Appl. Phys. 74 (2016) 6.
GAPS collaboration, Astropart. Phys. 145 (2023) 102791
F. Calore et al., SciPost Phys. 12 (2022) 16

AMS-02 & GAPS: DETECTING ANTINUCLEI

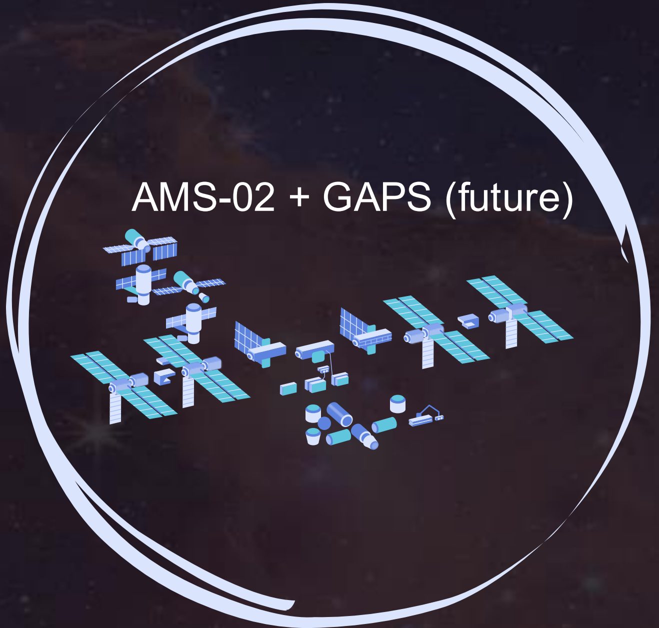

Detection

- The **Alpha Magnetic Spectrometer** (**AMS**) detector is designed to operate as an external module on the ISS
- To this day, the AMS-02 data (latest release: 2021) of cosmic antiprotons are very well **fitted by the secondary component**
- **No antideuteron** signal confirmed yet

AMS collaboration, Phys. Rev. Lett. 117 (2016) 091103
AMS collaboration, Phys. Rept. 894 (2021)
T. Aramaki et al., GAPS, Appl. Phys. 74 (2016) 6.
GAPS collaboration, Astropart. Phys. 145 (2023) 102791
F. Calore et al., SciPost Phys. 12 (2022) 16

AMS-02 & GAPS: DETECTING ANTINUCLEI

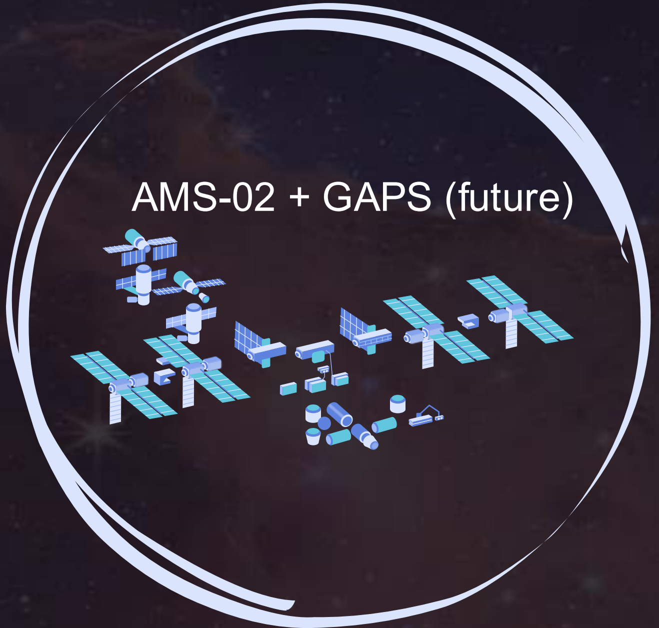

Detection

- The **Alpha Magnetic Spectrometer** (**AMS**) detector is designed to operate as an external module on the ISS
- To this day, the AMS-02 data (latest release: 2021) of cosmic antiprotons are very well **fitted by the secondary component**
- **No antideuteron** signal confirmed yet
- **GAPS** (**General AntiParticle Spectrometer**) is an Antarctic balloon mission that will search for low-energy (< 0.25 GeV/n) cosmic-ray antinuclei in the future

2202.03076

AMS collaboration, Phys. Rev. Lett. 117 (2016) 091103
AMS collaboration, Phys. Rept. 894 (2021)
T. Aramaki et al., GAPS, Appl. Phys. 74 (2016) 6.
GAPS collaboration, Astropart. Phys. 145 (2023) 102791
F. Calore et al., SciPost Phys. 12 (2022) 16

AMS-02 & GAPS: DETECTING ANTINUCLEI

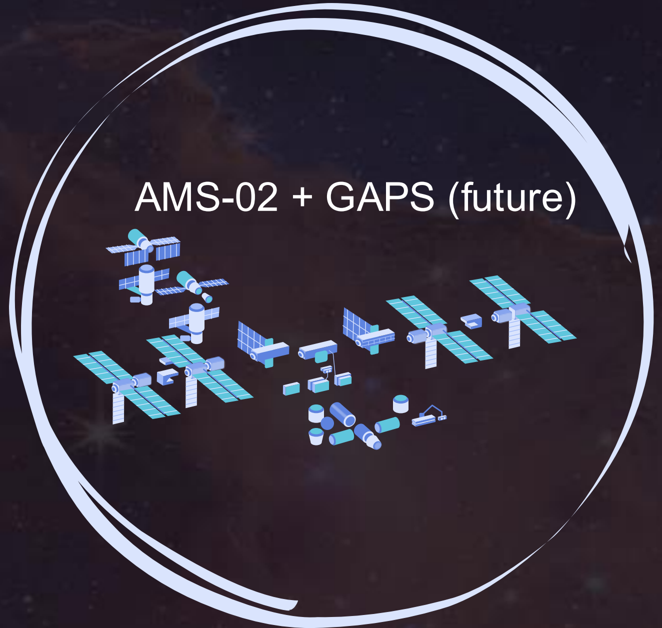

Detection

- The **Alpha Magnetic Spectrometer** (**AMS**) detector is designed to operate as an external module on the ISS
- To this day, the AMS-02 data (latest release: 2021) of cosmic antiprotons are very well **fitted by the secondary component**
- **No antideuteron** signal confirmed yet
- **GAPS** (**General AntiParticle Spectrometer**) is an Antarctic balloon mission that will search for low-energy (< 0.25 GeV/n) cosmic-ray antinuclei in the future
- GAPS would be sensitive to the **low-energy tail** in which the PBH contribution to antinuclei is more prominent

AMS collaboration, Phys. Rev. Lett. 117 (2016) 091103
AMS collaboration, Phys. Rept. 894 (2021)
T. Aramaki et al., GAPS, Appl. Phys. 74 (2016) 6.
GAPS collaboration, Astropart. Phys. 145 (2023) 102791
F. Calore et al., SciPost Phys. 12 (2022) 16

COMPUTATIONAL ASPECTS AND STATYSTICAL ANALYSIS

1 Through **BlackHawk**, we compute the Hawking radiation from a population of **PBHs** with a **lognormal mass distribution**, for different μ_c and σ

2 We derive the antiproton emission with **CosmiXs** from quarks and bosons

3 We propagate the $\bar{p}$ flux with **USINE** in the **BIG** configuration

4 By comparing with AMS-02 2021 data, we derive **UL PBH densities** at 95% CL

5 We evaluate the antideuteron primary fluxes using the Argon-Wigner coalescence of **CosmiXs** and applying the antiproton density bounds.

Y. Genolini et al., PRD 99 (2019) 123028
M. Boudaud et al., Phys. Rev. Res. 2 (2020) 02302
F. Calore et al., SciPost Phys. 12 (2022) 16
A. Arbey et al., Eur. Phys. J. C 79 (2019) 693
C. Arina et al., JCAP 03 (2024) 035
M. Di Mauro et al., 2411.04815
D. Maurin, Communications 247 (2020) 106942

RESULTS

ANTIPROTON FLUXES

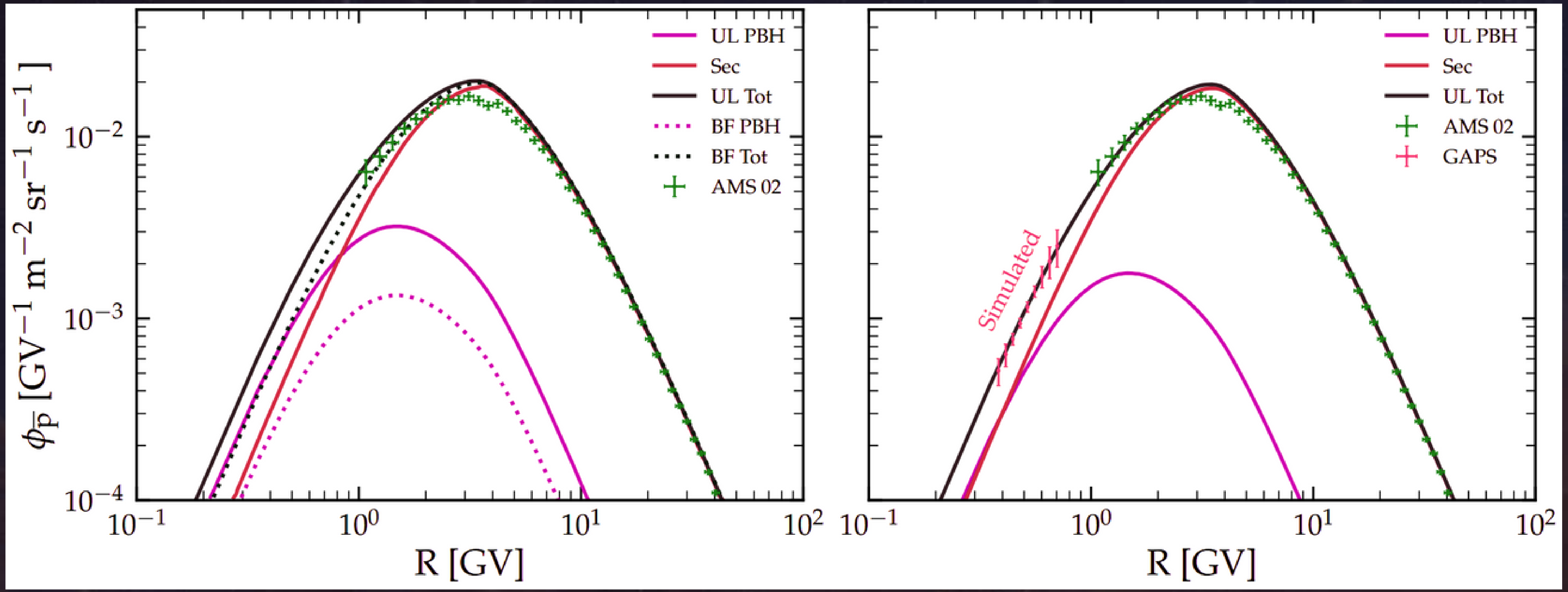

- The **Upper Limit** (**UL**) is evaluated at 95% C.L. with **AMS-02 2021 data only** (left) and adding **GAPS simulated** data (right)
- AMS-02 2021 data are well fitted by the secondary contribution → **suppressed PBH contribution**

AMS collaboration, Phys. Rept. 894 (2021)
GAPS collaboration, Astropart. Phys. 145 (2023) 102791
F. Calore et al., SciPost Phys. 12 (2022) 163

ANTIPROTON FLUXES

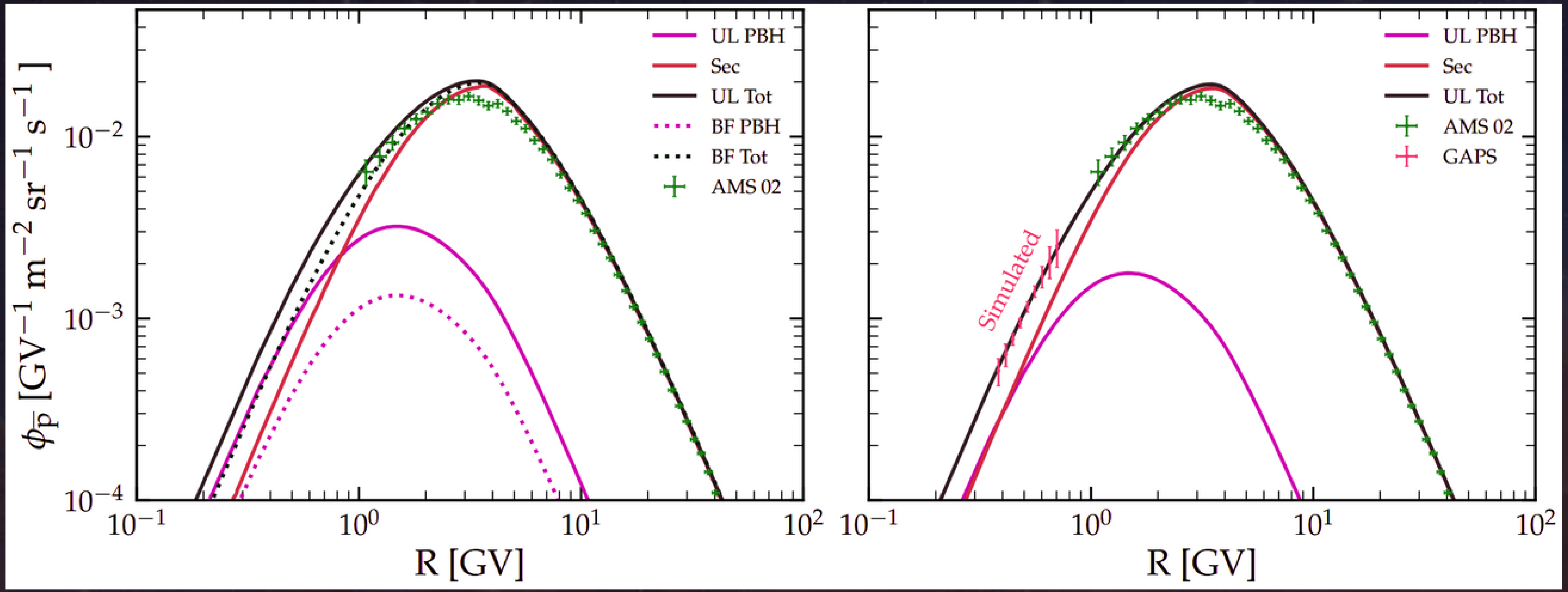

- The **Upper Limit** (**UL**) is evaluated at 95% C.L. with **AMS-02 2021 data only** (left) and adding **GAPS simulated** data (right)

- AMS-02 2021 data are well fitted by the secondary contribution → **suppressed PBH contribution**

- GAPS data would help to investigate the **low energy tail** where the PBH contribution is significant

AMS collaboration, Phys. Rept. 894 (2021)
GAPS collaboration, Astropart. Phys. 145 (2023) 102791
F. Calore et al., SciPost Phys. 12 (2022) 163

BOUNDS ON PBHs AS DM

$$f_{\mathrm{PBH}} = \frac{\rho_{\mathrm{PBH}}}{\rho_{DM}}$$

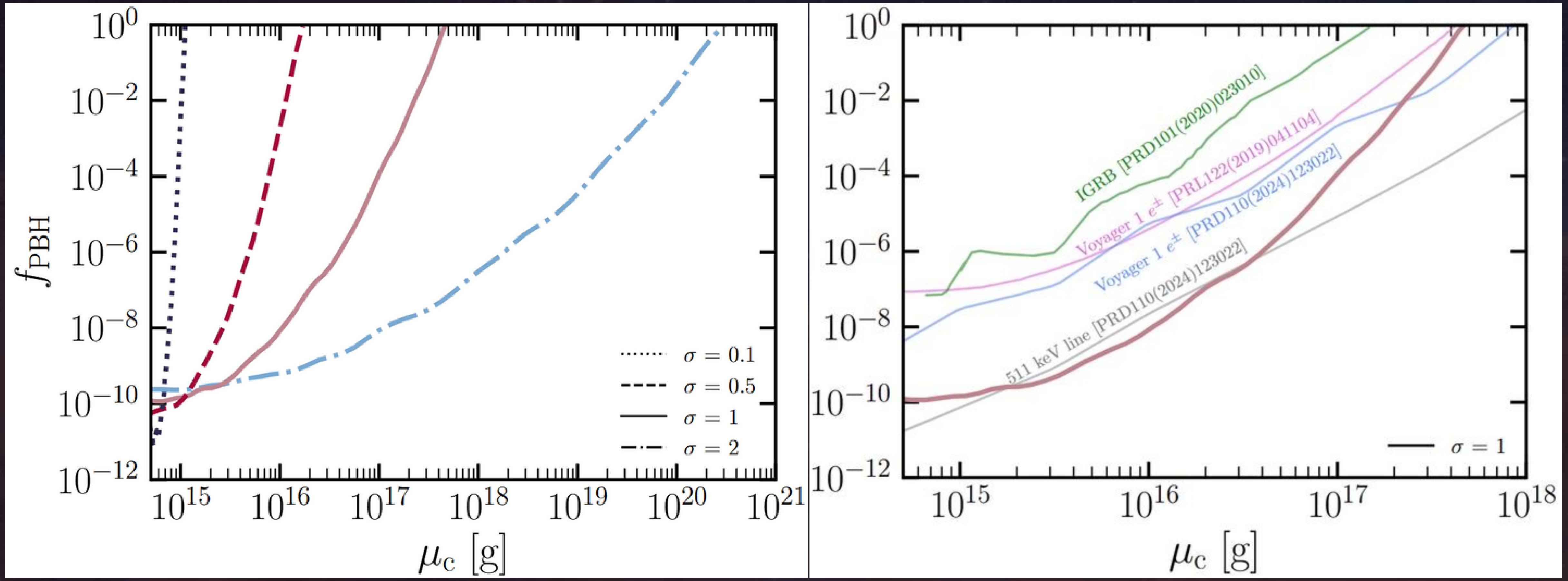

- 95% CL UL on ρ_{PBH} and f_{PBH} with **AMS-02 2021** data
- Higher widths imply that a bigger portion of the asteroid mass range is constrained, although the constraining power gets reduced with increasing mass

BOUNDS ON PBHs AS DM

$$f_{\rm PBH} = \frac{\rho_{\rm PBH}}{\rho_{DM}}$$

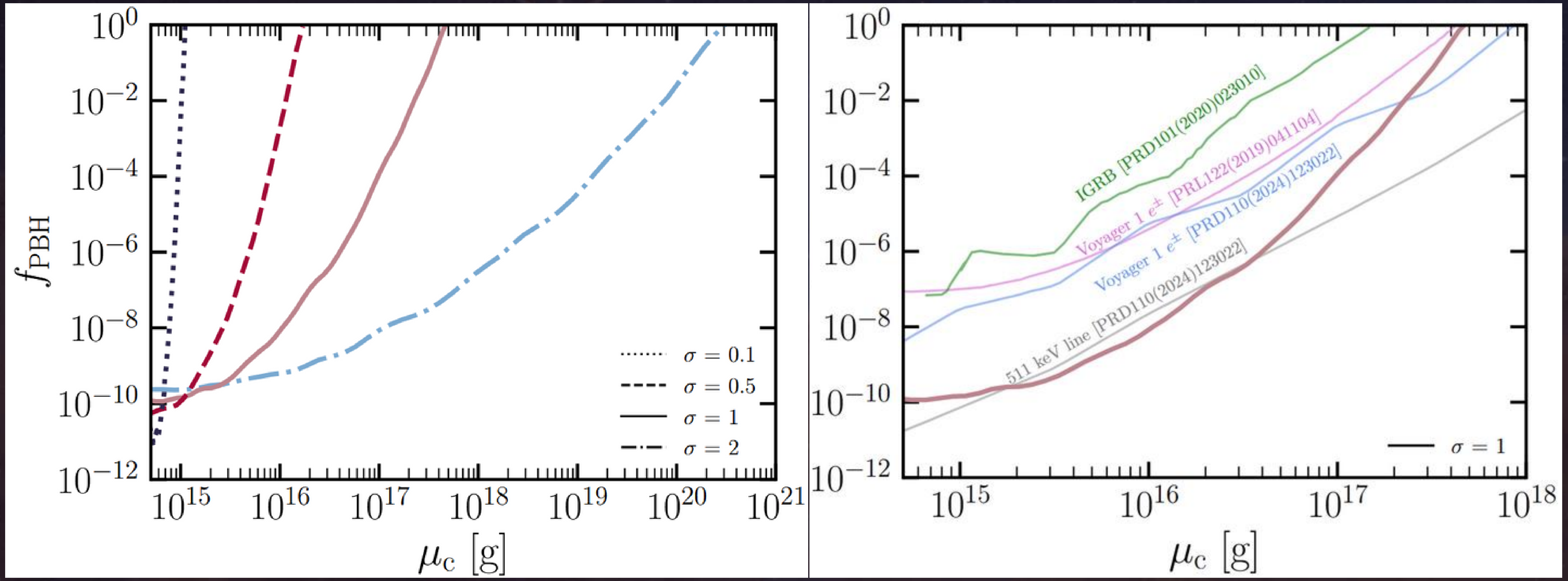

- 95% CL UL on $\rho_{\rm PBH}$ and $f_{\rm PBH}$ with **AMS-02 2021** data
- Higher widths imply that a bigger portion of the asteroid mass range is constrained, although the constraining power gets reduced with increasing mass
- Bounds are competitive to other multi-messenger constraints, although with different analysis

ESTIMATED ANTIDEUTERON FLUX

- We applied the **the previous UL densities from antiprotons**

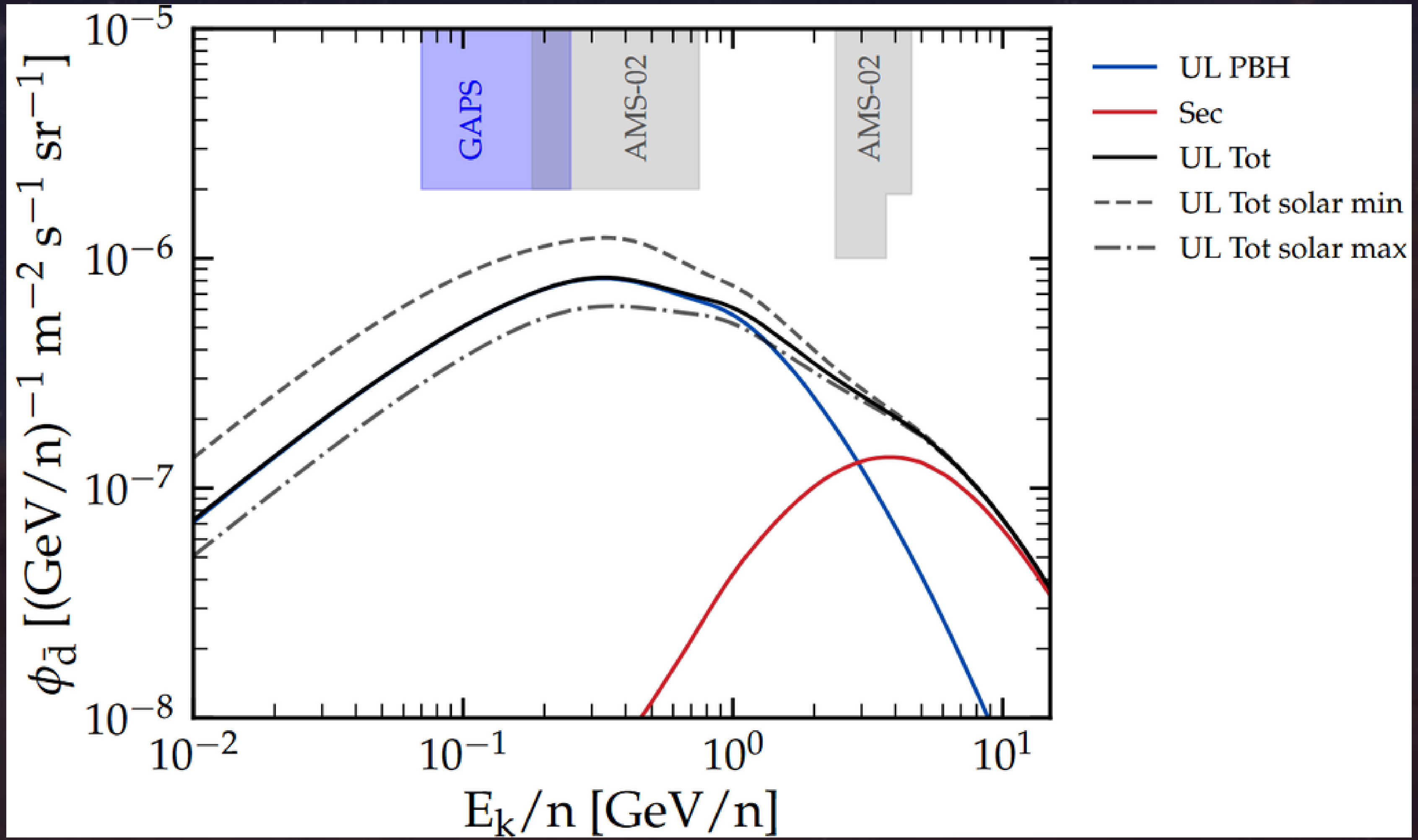

$$\mu_c = 10^{15} g$$

$$\sigma = 1$$

$$\rho_{\mathrm{PBH}} = 5.2 \times 10^{-11}\ \mathrm{GeV\ cm}^{-3}$$

M. Di Mauro, et al., 2411.04815

T. Aramaki et al., Appl. Phys. 74 (2016) 6

T. Aramaki, et al., Physics Reports 618 (2016) 1

ESTIMATED ANTIDEUTERON FLUX

- We applied the **the previous UL densities from antiprotons**
- The PBH contribution is more relevant than the secondary one below 3 GeV/n, but it is **far from GAPS** and **AMS-02** sensitivities, even taking into account different solar modulations

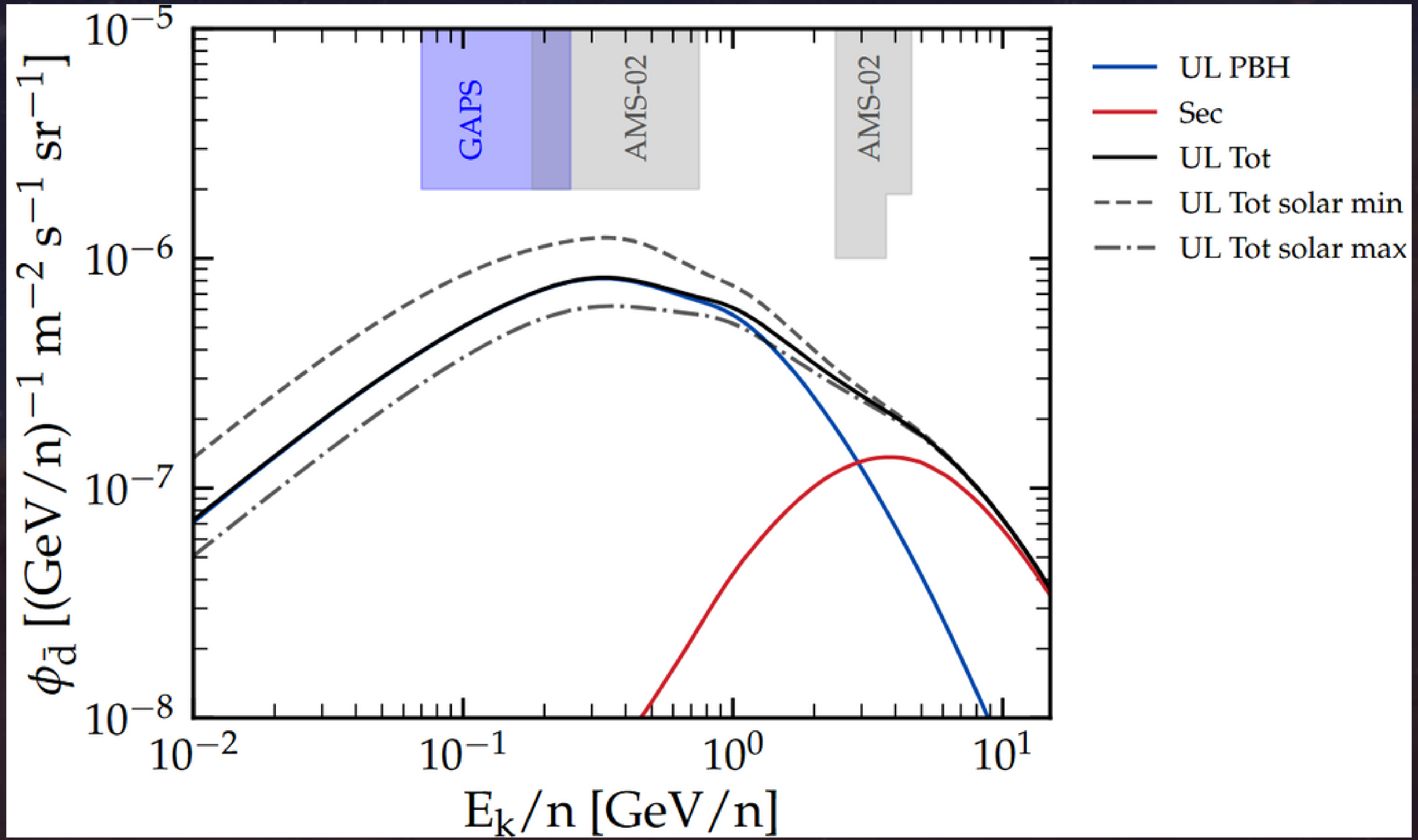

$$\mu_c = 10^{15} g$$

$$\sigma = 1$$

$$\rho_{\rm PBH} = 5.2 \times 10^{-11}\ {\rm GeV\ cm}^{-3}$$

M. Di Mauro, et al., 2411.04815

T. Aramaki et al., Appl. Phys. 74 (2016) 6

T. Aramaki, et al., Physics Reports 618 (2016) 1

ESTIMATED ANTIDEUTERON FLUX

- We applied the **the previous UL densities from antiprotons**
- The PBH contribution is more relevant than the secondary one below 3 GeV/n, but it is **far from GAPS** and **AMS-02** sensitivities, even taking into account different solar modulations
- If antideuterons were to be detected, they **could not be explainable by PBHs only** as BSM physics

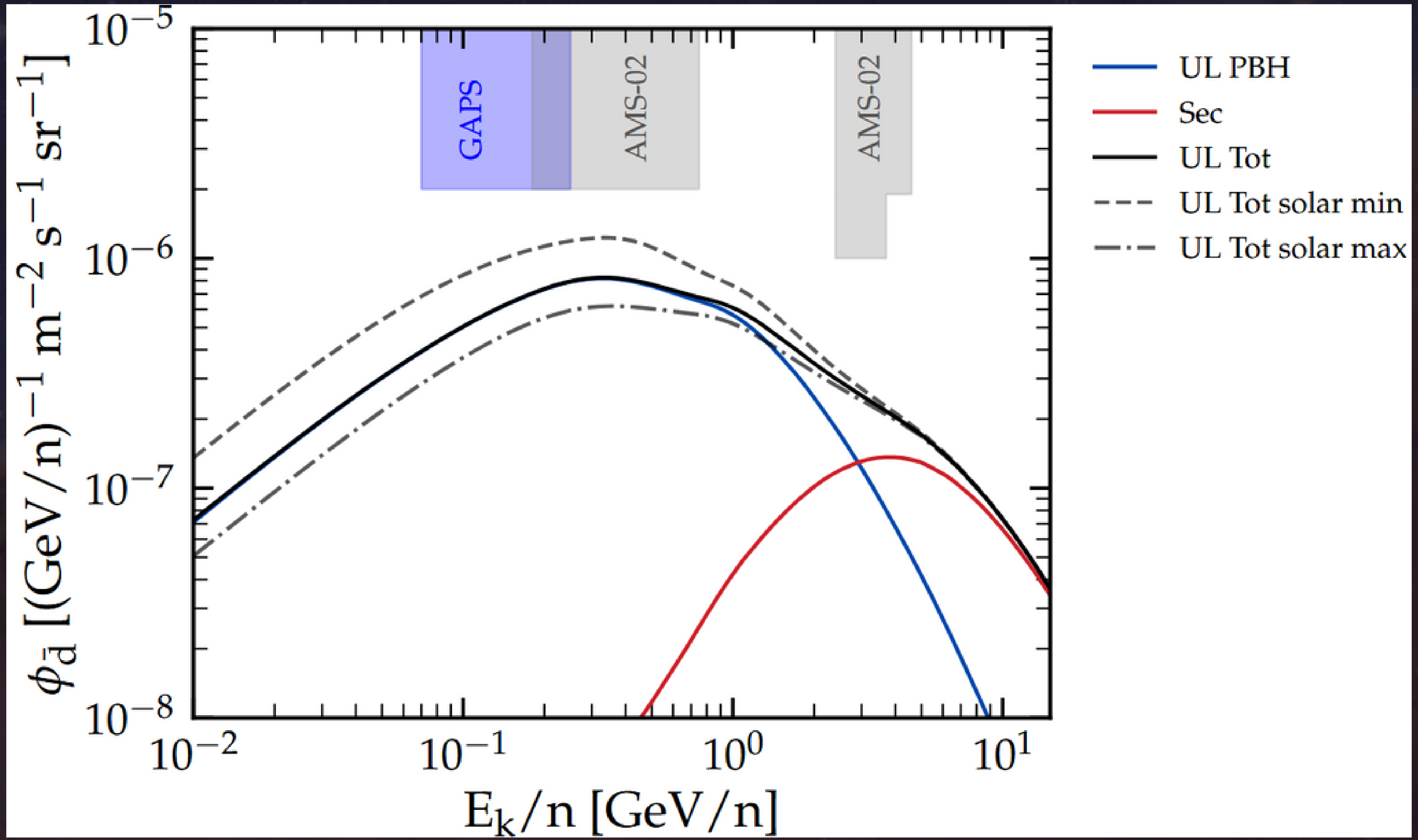

$$\mu_c = 10^{15} g$$

$$\sigma = 1$$

$$\rho_{\rm PBH} = 5.2 \times 10^{-11}\ \text{GeV cm}^{-3}$$

M. Di Mauro, et al., 2411.04815

T. Aramaki et al., Appl. Phys. 74 (2016) 6

T. Aramaki, et al., Physics Reports 618 (2016) 1

CONCLUSIONS

2505.04692
Phys. Rev. D 112 (2025) 2, 023003

- We revisited the CR antiproton and antideuterons signatures from PBH evaporation in the Galaxy
- We improved previous calculations by assuming a lognormal PBH mass distribution, using updated Galactic propagation parameters and the most recent AMS-02 antiproton data within a sophisticated statistical analysis
- We cast competitive bounds with antiprotons on $f_{\rm PBH}$ in the asteroid mass range
- We estimated that if one or more antideuterons were to be measured by AMS-02 or by GAPS, they would clearly be a signal of new physics, but not completely explainable with PBH emission

CONCLUSIONS

2505.04692
Phys. Rev. D 112 (2025) 2, 023003

- We revisited the CR antiproton and antideuterons signatures from PBH evaporation in the Galaxy
- We improved previous calculations by assuming a lognormal PBH mass distribution, using updated Galactic propagation parameters and the most recent AMS-02 antiproton data within a sophisticated statistical analysis
- We cast competitive bounds with antiprotons on f_{PBH} in the asteroid mass range
- We estimated that if one or more antideuterons were to be measured by AMS-02 or by GAPS, they would clearly be a signal of new physics, but not completely explainable with PBH emission

Thanks for your attention!

Questions?

BACKUP

ANTIPROTONS FROM BOSONS

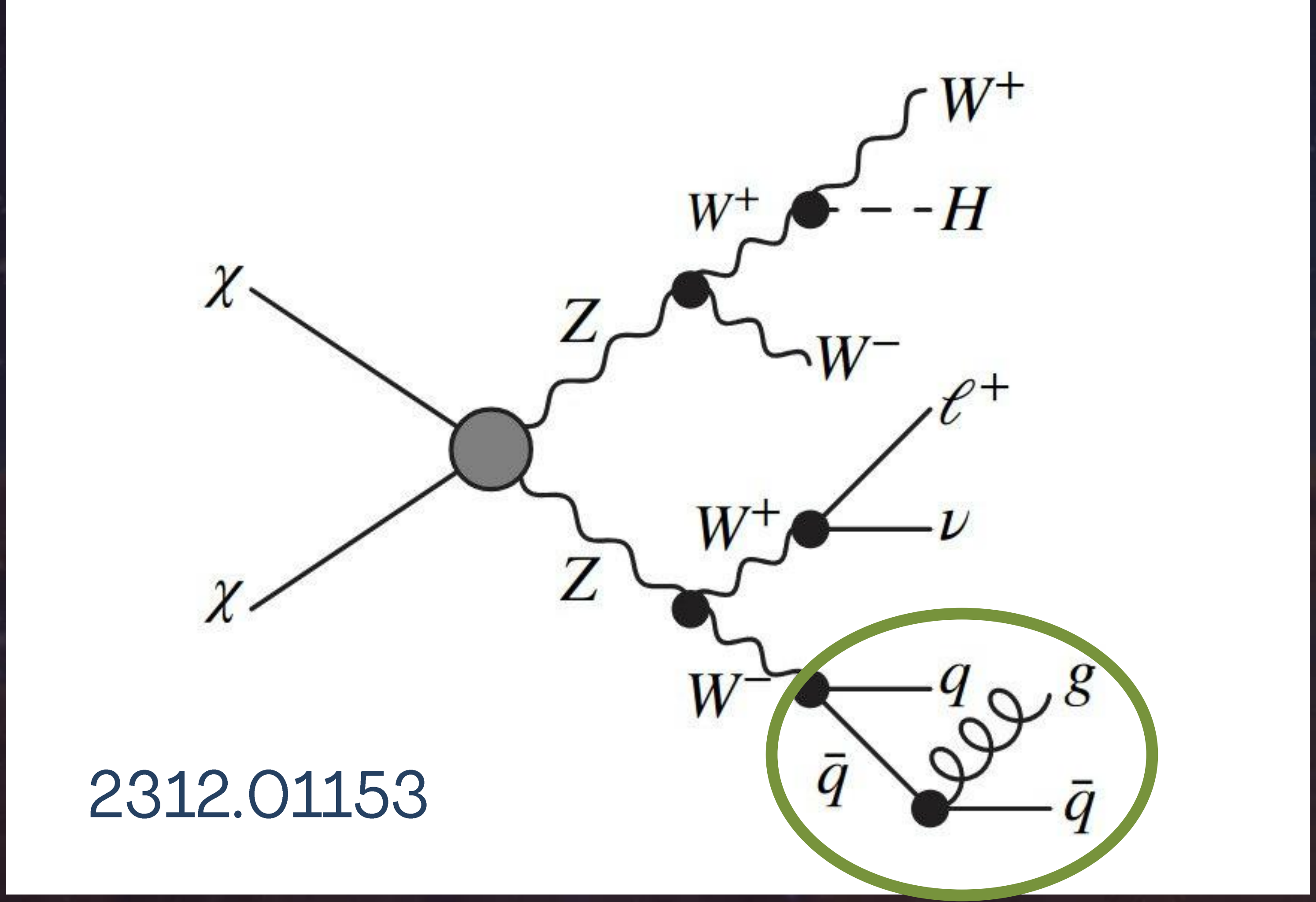

- Bosons can further produce quark – antiquark pair through EW processes, which hence might hadronize into antinuclei, for example

C. Arina et al, 2312.01153
M. Di Mauro et al., 2411.04815

COALESCENCE OF ANTIDEUTERONS

- Simple coalescence model

$$\Delta p = |\overrightarrow{p_{\bar{n}}} - \overrightarrow{p_{\bar{p}}}| \leq p_{coal}$$

  in the antideuteron rest frame
- Simple coalescence model with sharp distance cutoff $\boldsymbol{\Delta p, \Delta r \leq 3fm}$
- Wigner coalescence model with Gaussian distribution

$$D(\Delta r, \Delta p) \propto e^{-\Delta r^2 /(2\sigma^2)} e^{-\Delta p^2 \, \delta^2 \, /2}$$

  where σ and $1/\delta$ account for the Gaussian distribution widths for the antinuclei separations in space and momentum, around 2 fm

C. Arina et al, 2312.01153
M. Di Mauro et al., 2411.04815
M. Mahlein et al., Eur. Phys. J. C 83, 804 (2023)

- **Wigner formalism**

  The number of created deuterons with momentum P_d is given by projecting the deuteron density matrix onto the two-nucleon density matrix when the interactions cease and the coalescence can occur

  (See 2302.12696 for more)

Mahlein et al., 2023

$$\frac{dN_\mathrm{d}}{d^3P_\mathrm{d}} \sim \frac{1}{2!}\int d^3x_1\, d^3x_2\, d^3x_1'\, d^3x_2'\, \phi_\mathrm{d}^*(\boldsymbol{x}_1, \boldsymbol{x}_2)\, \phi_\mathrm{d}(\boldsymbol{x}_1', \boldsymbol{x}_2') \times \left\langle \psi^\dagger(\boldsymbol{x}_2', t_\mathrm{f})\, \psi^\dagger(\boldsymbol{x}_1', t_\mathrm{f})\, \psi(\boldsymbol{x}_1, t_\mathrm{f})\, \psi(\boldsymbol{x}_2, t_\mathrm{f}) \right\rangle . \quad (3.5)$$

M. Mahlein et al., Eur. Phys. J. C 83, 804 (2023)

- Argonne – Wigner coalescence model:

Hence, the deuteron spectrum takes the form

$$\gamma \frac{\mathrm{d}N_\mathrm{d}}{\mathrm{d}^3P} = \frac{S_\mathrm{d}}{(2\pi)^4} \int \mathrm{d}^4 r_\mathrm{d} \int \frac{\mathrm{d}^4 q}{(2\pi)^4} \int \mathrm{d}^4 r \, \tilde{\mathcal{D}}(q, r) \times \times f_1^W \left(P/2 + q, r_\mathrm{d} + \frac{r}{2}\right) f_1^W \left(P/2 - q, r_\mathrm{d} - \frac{r}{2}\right), \quad (5)$$

where we define the relativistic internal Wigner density as

$$\tilde{\mathcal{D}}(q, r) = \int \mathrm{d}^4 \xi \, e^{iq\xi} \varphi_\mathrm{d} \left(r + \frac{\xi}{2}\right) \varphi_\mathrm{d}^* \left(r - \frac{\xi}{2}\right). \quad (6)$$

Mahlein et al., 2023

M. Mahlein et al., Eur. Phys. J. C 83, 804 (2023)

COALESCENCE OF ANTIDEUTERONS

- Argonne - Wigner coalescence model: implemented for the first time in 2312.01153, Wigner formalism with v18 Argonne potential

The Argonne v_{18} potential is a phenomenological potential for the deuteron, tuned through p–p and n–p inelastic scattering data, low-energy $n-n$ scattering parameters, and deuteron binding energy [36]. In such a potential, the deuteron wavefunction has the form:

$$\varphi_{\mathrm{d}}(\vec{r}) = \frac{1}{\sqrt{4\pi} r}\left[u(r) + \frac{1}{\sqrt{8}} w(r) S_{12}(\hat{r})\right] \chi_{1m}, \tag{S9}$$

where $S_{12}(\hat{r}) = 3\,(\vec{\sigma}_1 \cdot \vec{r})\,(\vec{\sigma}_2 \cdot \vec{r}) - (\vec{\sigma}_1 \cdot \vec{\sigma}_2)$ is the spin tensor, σ_i are the Pauli matrices, χ_{1m} is a spinor, and $u(r)$ and $w(r)$ are radial S and D wavefunctions, respectively. The wavefunction is normalised as follows:

$$\int \mathrm{d}^3 r\, |\varphi_{\mathrm{d}}(\vec{r})|^2 = \int \mathrm{d}^3 r \frac{1}{4\pi r^2}\left[u^2(r) + w^2(r)\right] = 1.$$

We have tabulated the Wigner function $\mathcal{D}(r,q)$ found with the Argonne wavefunction as a function of r and q following the fit presented in [47].

2312.01153

M. Di Mauro et al., 2312.01153

COALESCENCE OF ANTIDEUTERONS

- Argonne – Wigner coalescence model: implemented for the first time in 2411.04815, Wigner formalism with v18 Argonne potential

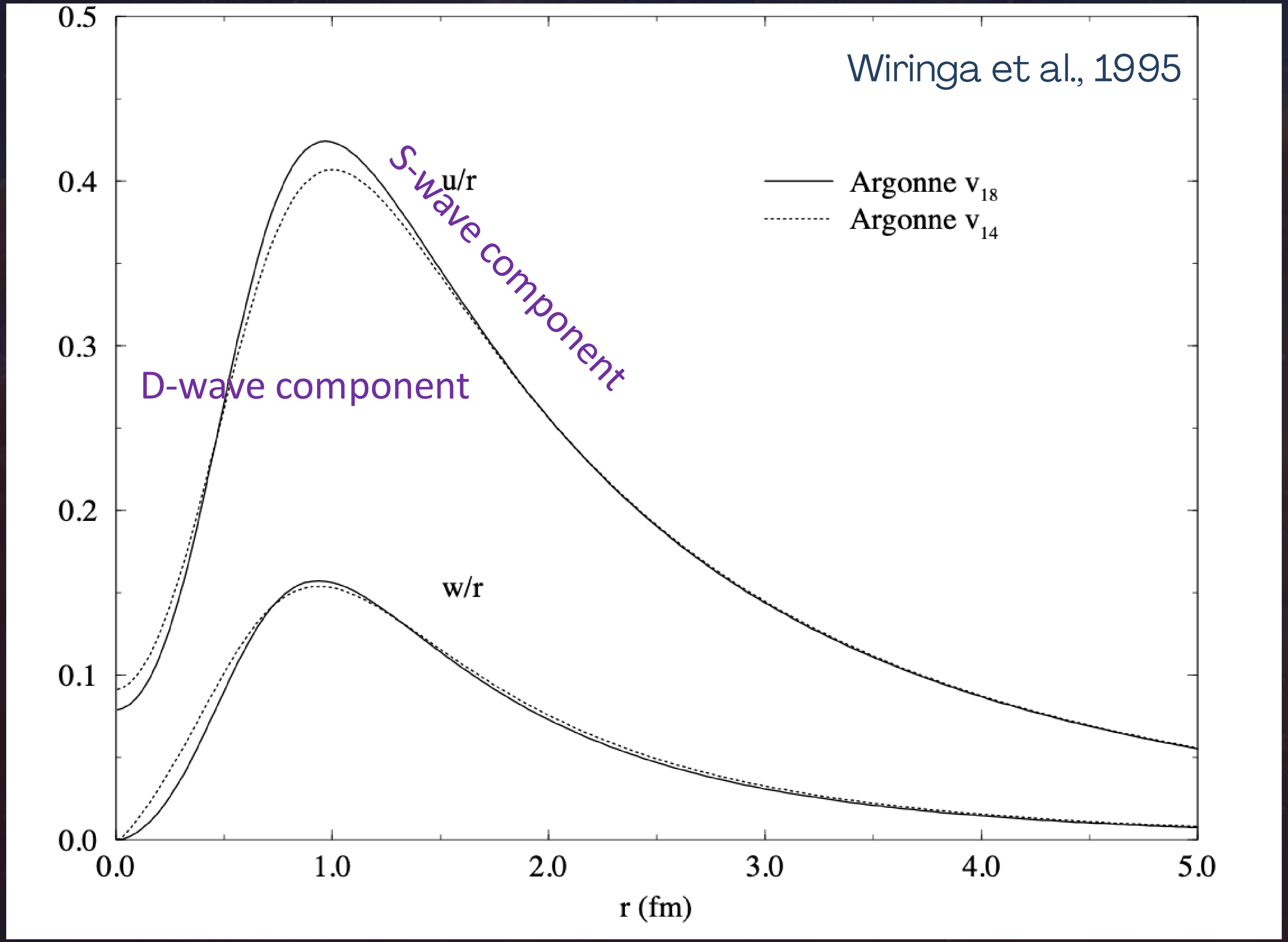

R.B. Wiringa et al., Phys. Rev. C 51, 38 (1995)

PROPAGATION – COMPLETE EQUATION

The complete transport equation contains

- spatial and momentum diffusion terms
- reacceleration and energy loss terms
- convective galactic wind terms
- Primary, secondary and tertiary source terms
- Depletion by spallation term

$$
-\left[K\left(\frac{\partial^2}{\partial z^2}+\frac{1}{r}\frac{\partial}{\partial r}\left(r\frac{\partial}{\partial r}\right)\right)-V_c\frac{\partial}{\partial z}\right]n+2h\,\delta(z)\frac{\partial}{\partial E}\left[b(E)\,n-c(E)\,\frac{\partial n}{\partial E}\right]
$$
$$
= q^{\mathrm{prim}}(E)+2h\delta(z)\left[q^{\mathrm{sec}}(E)+q^{\mathrm{ter}}(E)\right]-2h\,\delta(z)\sum_{t\in\mathrm{ISM}} n_t v\,\sigma_{\mathrm{inel}}\,n\,.
$$

2505.04692

See also F. Calore et al., SciPost Phys. 12 (2022) 16

STATYSTICAL ANALYSIS

$$-2\ln\mathcal{L}(L,\mu) = \sum_{i,j} x_i(\mathcal{C}^{-1})_{ij}x_j + \left\{\frac{\log L - \log\hat{L}}{\sigma_{\log L}}\right\}^2 \,,$$

2505.04692

- To fasten the analysis, the likelihood is split in two components: one, with the covariant matrix C, that fully encloses the uncertainty on the transport parameters (left; fully embodied by the secondary component, that is dominant); one that represents the uncertainty on the halo size L, that mainly affects the primary component
- μ represents the primary component free parameter (DM mass, PBH mass…)
- x_i represents the difference between the experimentally-measured fluxesand the predicted ones

$$x_i \equiv \psi_i^{\text{exp}} - \psi_i^{\text{th}}(L,\mu),$$

F. Calore et al., SciPost Phys. 12 (2022) 16